J. Phys. B: At. Mol. Phys. **19** (1986) 4035-4050. Printed in Great Britain

Total cross sections for low and intermediate energy positrons and electrons colliding with CH_4, C_2H_4 and C_2H_6 molecules

O Sueoka and S Mori

Institute of Physics, College of Arts and Sciences, University of Tokyo, 3-8-1 Komaba, Meguro-ku, Tokyo 153, Japan

Received 6 August 1985, in final form 2 April 1986

Abstract. Total cross sections for 0.7-400 eV positrons and 1.0-400 eV electrons colliding with CH_4, C_2H_4 and C_2H_6 molecules have been measured using a retarding potential-TOF (RP-TOF) method. The cross sections were obtained by a normalisation method rather than absolute measurements. The minima of the total cross sections for positron scattering by these hydrocarbons were distinctly shown in the region from 4 to 5 eV. The total cross sections for electron collisions with these hydrocarbons were compared with previous data and with positron collision data.

1. Introduction

A number of measurements of total cross sections for low- and intermediate-energy positrons colliding with atoms and molecules have been performed recently (Griffith 1979, Kauppila and Stein 1982). Some of these results were compared with data for electron collisions obtained by the same apparatus and techniques. The interaction of positrons with atoms and molecules has been understood fairly well through many experimental and theoretical studies. For all the positron collision measurements with atoms and molecules, results for the total cross section do not show any resonance-like structure, while for electron collisions it is well known that shape resonances exist in many molecules at low energies and Feshbach-type resonance exists in rare gases at energies just below the excitation energy. On the other hand, a total cross section curve for positron collisions varies more smoothly than that for electron collisions and no resonance has been observed. Recently, Mizogawa *et al* (1985) have shown, by a precise TOF measurement, that resonance was not observed in e^+-He.

In the present paper, measurements of total cross sections for positrons colliding with the hydrocarbon molecules CH_4, C_2H_4 and C_2H_6 were performed in the same framework as that in our previous work on $e^{\pm}$-N_2, $e^{\pm}$-CO and $e^{\pm}$-CO_2 (Sueoka and Mori 1984a). As methane (CH_4) molecules are important in various applications, they have been studied by several kinds of electron collision experiment and by theoretical calculations. It was necessary to perform the measurement for e^+-CH_4 again because the values of the cross section of Kauppila *et al* (1983) and Charlton *et al* (1983) in the vicinity of the minimum show a large discrepancy with each other. Data for e^+-CH_4 were compared with the experimental data of Charlton *et al* (1980, 1983), Kauppila *et al* (1983) and Floeder *et al* (1985).

Total cross sections for positrons colliding with ethylene (C_2H_4) and ethane (C_2H_6) molecules have also been compared with the recent results of Floeder *et al* (1985) in

the range from 5 to 400 eV. We also take an interest in positron scattering by C_2H_4, as C_2H_4 molecules with a double bond show a shape resonance at 2.0 eV in electron collision measurements. One of the purposes of this work is to search for the effect of the double bond (C=C) on positron scattering.

For these hydrocarbon molecules, the total cross section Q_t for electrons was also measured. The results for e^--CH_4 were compared with previous experimental data and theoretical results. For e^--C_2H_4 and e^--C_2H_6 results were compared with the experimental data of Brüche (1929, 1930) and Floeder *et al* (1985).

Some of the present data have been reported elsewhere (Sueoka and Mori 1984b).

2. Experimental procedure

The apparatus, positron and electron beam sources, electronics and methods of data analysis used in this experiment are nearly the same as those described in a previous paper (Sueoka and Mori 1984a). The schematic diagram of the apparatus and main electronic circuits is shown in figure 1. The diameters of the two apertures of the cell and that of the holes for differential pumping are 8 mm. The gas pressure was measured using a Baratron gauge replaced by a Convectron and a Hg-MacLeod gauge system that was used in the previous work. The effective length of the collision cell, l, is 71.7 mm, larger than the geometrical length by 6%. The value of l was not obtained directly, but was determined from the normalisation of the total cross section to the data of Hoffman *et al* (1982) for e^+-N_2. The change of the effective length from the previous value 79.7 mm is mainly due to lack of accuracy in the previous pressure measurement system and not due to the geometrical factor. The effective length is not an important factor in our normalisation measurement because the value is determined using the assumption that the scale in the pressure gauge is correct. Radioactive ^{22}Na with an activity of about 60 μCi was used as a positron source. A moderator of tungsten ribbon was used. As an electron source, ^{137}Cs with activity of 40 μCi using the same

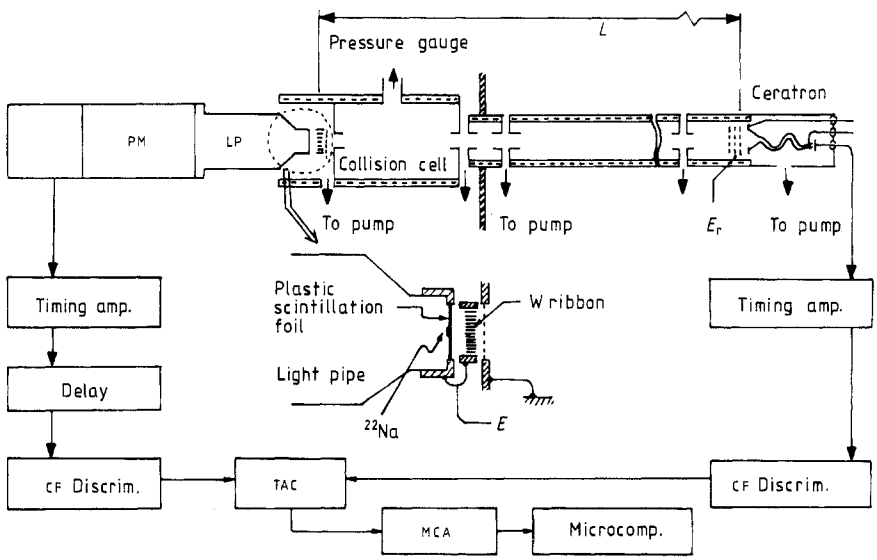

Figure 1. Schematic diagram of the experimental arrangement and the timing electronics.

moderator was adopted. The intensity and the spectrum of the projectile particle sources depend on the contamination of moderator surfaces and on the spacing geometry of the tungsten ribbon of the moderator. The electron and positron spectra are presented in figure 2. (The spectrum is not altered by the energy resolution of the TOF spectrometer.) Beam intensities of less than 1 eV, as shown in the 0 eV spectrum, decrease in transportation along the flight path by the characteristics of the spectrometer. The number of slow positrons is about 3.5 $e^+ s^{-1}$ in good conditions and 1.5 $e^+ s^{-1}$ in lower energy regions. On the other hand, the conversion efficiency to slow positrons is deduced to be 1×10^{-4} in the vicinity of the moderator.

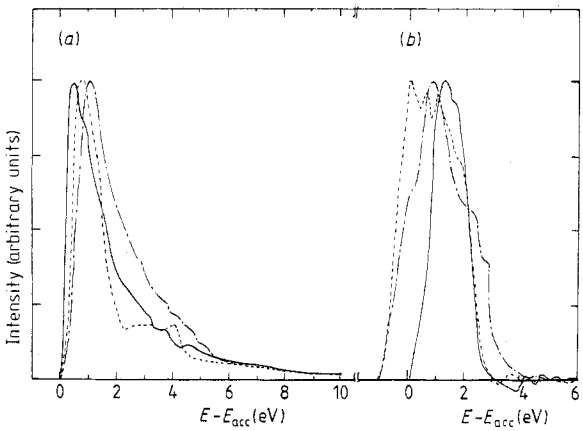

Figure 2. (*a*) Spectra of slow electrons for acceleration energies of 0(0) (——), −6(−6) (- - -) and −17.4(−17.4) (— · —) eV; (*b*) spectra of slow positrons for 0(0) (——), 1.5(0) (- - -) and 18.5(17.0) (— · —) eV. The number in parentheses is the retarding potential in eV. These spectra were corrected by the retarding potential. Hump-like irregularities in the −6 eV electron spectrum, and the 1.5 and 18.5 eV positron spectra are due to the magnetic field.

Projectile particles were guided by a magnetic field by means of solenoid coils surrounding the collision cell and the flight path. The magnetic field at the cell was 9 G for positron collision measurements. For electrons, the field was decreased to 4.5 G, though the field was 9 G in the preliminary experiments (Sueoka and Mori 1984b).

Positron measurements with a 4.5 G magnetic field were performed and compared with those at 9 G at several energy points only. The results for positron collisions are given, along with those for electrons, in figure 3. Total cross sections for the two conditions coincide with each other in the range above about 3 eV. At low energies, experimental results show that some of the scattered positrons are detected with the 9 G field. Unfortunately, for our experimental set-up it is difficult to perform all the positron measurements with a field of 4.5 G. However, it was shown by theoretical work of Jain (1983) that the differential cross section for positron collisions with CH_4 did not present sharper forward peaking than that of electron collisions at 25–800 eV.

As shown in figure 3, the ratios of '9 G' to '4.5 G' in the electron experiment were less than one in energy ranges below 1.6 eV and from 15–60 eV, which suggests the possibility that the cross sections increase with decreasing magnetic field. To assure the validity of 4.5 G measurements for electrons, the following measurements were carried out. First, a further check of the magnetic field dependence at 1–3 eV was

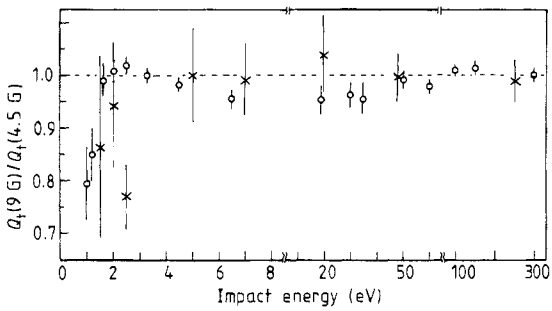

Figure 3. Ratio of total cross sections with a magnetic field of 9 G at the vicinity of the collision cell, to those at 4.5 G for electron (○) and positron (×) collision measurements. The low values of the ratio mean that the total cross section, Q_t, decreases due to the mixture of scattered particles to unscattered ones.

performed, as shown in figure 4. Though the data at an impact energy of 1 eV were not statistically accurate enough, the same dependence of the cross section values on magnetic field was obtained at each energy. The results in figures 3 and 4 are consistent. To confirm the validity of the 15-60 eV results, the measurements described above were performed at 30 eV and no significant change of the cross section values with a lower magnetic field was observed. In conclusion, for electron collisions the present total cross section data at 4.5 G are hardly affected by the magnetic field.

The retarding potential-time of flight (RP-TOF) of Sueoka (1982) was applied to eliminate the contribution of large-energy-loss inelastic collisions and to decrease the influence from the forward scattering due to elastically scattered positrons with reduced axial velocity resulting from angular deflection. The values of the retarding potential were selected 1.5 eV lower than the accelerating potential E_{acc} for positrons and were selected to be the same as E_{acc} for electrons, as in the previous work. The raw RP-TOF spectrum is deformed from the conventional TOF spectrum due to the decrease in the particle speed caused by the retarding voltage applied. RP-TOF spectra were corrected by taking this effect into account. Using a reasonable potential in the retarding area, however, raw RP-TOF spectra were fully corrected. Data at the lower energy were not

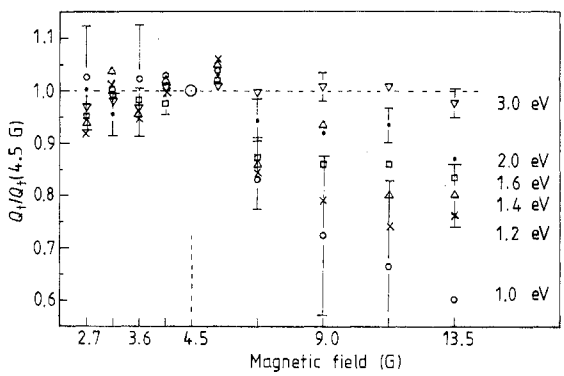

Figure 4. Ratio of the total cross sections with various magnetic fields at the vicinity of the collision cell, to that with 4.5 G, for impact energies of 1-3 eV in electron collision measurements. Impact energies: ○, 1.0 eV; ×, 1.2 eV; △, 1.4 eV; □, 1.6 eV; ●, 2.0 eV; ▽, 3.0 eV.

used in the calculation of the total cross sections due to the larger effect of the forward and inelastic scattering.

The typical run time for a datum point is 2 h for electron measurements and 4 h for positrons, in the higher energy regions, and in the lower regions 3 and 10 h, respectively. A vacuum run and a gas run were alternated in 500 s automatically.

The total cross section Q_t is computed from

$$Q_t = \frac{1}{\rho l} \ln\left(\frac{I_v}{I_g}\right) \tag{1}$$

where ρ is the gas density in the collision cell, l is the effective length of the cell, and I_v and I_g are intensities in the vacuum and gas runs, respectively.

The measurements to check the independence of the effective length of the collision cell with cell pressure and gas species were performed with electron and positron beams for CH_4, C_2H_4, C_2H_6 and N_2 molecules, as shown in figure 5. The pressure dependence of the effective length was hardly observed within the error. For a short

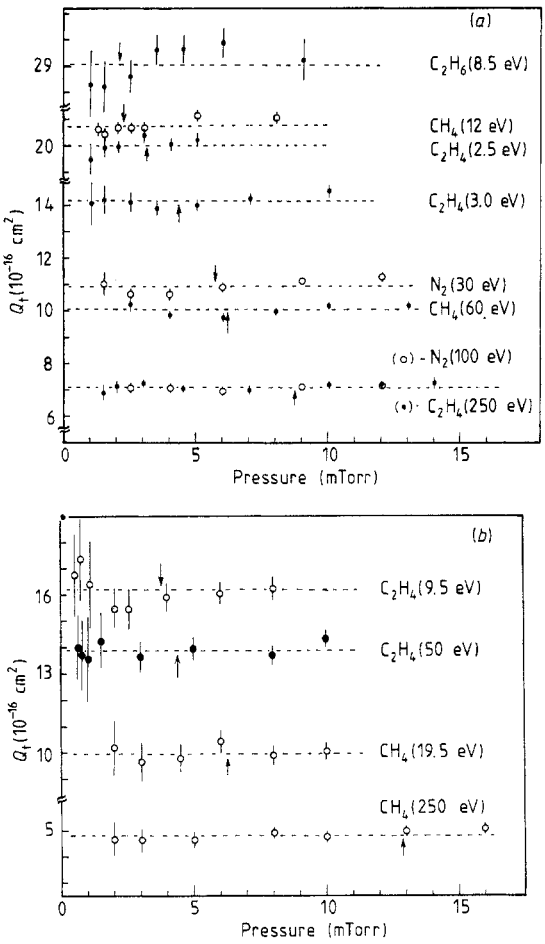

Figure 5. Total cross sections plotted against pressure for (*a*) electrons and (*b*) positrons for the four gases. The beam intensity attenuation (I_v/I_g) of 3.5 is shown by arrows. Measurements in practical cases were performed in the range between 3 and 4.

collision cell, however, a slight dependence may exist. The difference between the cross sections observed with the pressure used for the e^+-N_2 normalisation experiments (around 10 mTorr) and with the lower pressure used practically, where the beam attenuation is 3-4, is estimated to be at most 2%. We carried out measurements for these gases at many other energies as well.

Because the moderator in the present set-up is placed near the gas cell, the effect of background gas on the efficiency of slow-positron production must be checked. The authors suppose that the effect is independent of gas pressure. For slow-electron production, the effect may not exist. If the effect exists for positrons (it is not known whether the effect of anomalous production by a change in the state of the moderator surface is positive or negative), total cross sections are markedly changed at low pressures (namely, the attenuation value I_v/I_g, is near one), due to a larger change in the value of $\ln(I_g \pm \alpha I_g)/I_v$ against that of $\ln(I_g/I_v)$, where α is the ratio of the effect on the anomalous ejection of low-energy particles. No significant effect on Q_t values in low-pressure measurements (in measurement of both positron and electron scattering) was consistently found. In particular, the anomalous production effect was not shown consistently on low-energy data for C_2H_4 (50 and 9.5 eV). Therefore, we conclude that there as no serious effect on the production efficiency.

The evaluation of errors was the same as in the previous work. Namely the relative error, $\Delta Q_t/Q_t$, was obtained by linear addition of $\Delta I/I$, $\Delta\rho/\rho$ and $\Delta l/l$, where I means $\ln(I_v/I_g)$. The statistical error due to the beam intensity in the measurement of total cross sections ($\Delta I/I$) was 1.8-5.0% for positron experiments and 0.8-1.5% for electron experiments involving the error by subtraction of the accidental coincidences in each channel. Only the datum point at the lowest energy includes an error larger than the error value above. Errors due to the pressure measurement were determined by the same method as in the previous work. In particular, errors for C_2H_4 were large. Errors due to the normalisation for the determination of the effective length l, Δl, were 3%, and this value involves systematic uncertainties estimated by reproducibility for independent measurements.

Systematic uncertainties due to forward scattering were not counted. These may not be large, as indicated in the measurements related to figures 3 and 4. The error in the experiment of Hoffman *et al* (1982), of 17.5%, was added as the systematic error. This value is the maximum error, including the error due to forward scattering, with the experimental errors being 6% in their measurement.

The effect of the wide high tail in e^- beams on total cross sections is discussed next. The inelastically and elastically scattered parts of the tail electrons in the forward direction, in the region of the main part of the spectrum, contribute to diminishing cross sections. For simplification, we restrict ourselves to estimating the difference of the contribution for e^- beams from that for e^+ beams which do not have the tail. It is roughly estimated that the diminishing rate of total cross sections is less than 4%, though the rate depends on impact energy and gas species. This rate is rather small for the following reasons. (i) e^- and e^+ beams are accelerated by the ground potential in the same way because the electric field does not affect the interspaces of the W ribbons. (ii) The Feshbach resonance in e^--He (19.36 eV) was clearly detected by the precise TOF measurement of Mizogawa *et al* (1985) in which the e^- source and moderator used were of the same kind as ours. (iii) The retarding potential in $E_0 = 0$ was applied. (iv) Only the channels around the peak in the time spectrum were used for the calculation of cross sections. On the other hand, a proof that this estimation is not groundless is seen in figure 5. If the gas pressure is higher, cross sections decrease

because the portion of scattered contribution from the tail part in the main region increases. The variation of the cross sections with gas pressure show a slightly reversed tendency. The tendency for e^- is almost the same as that for e^+, as shown in the figure.

The impact energy in the electron experiments was corrected by means of the addition of 0.6 eV as $E_\perp$ to $E_\parallel$, where $E_\perp$ and $E_\parallel$ mean the energy perpendicular and parallel to the direction of the flight pipe, respectively. This value (0.6 eV) was obtained through the observation of the energy shift of the shape resonance in electron scatterings by N_2, CO and CO_2.

Secondary electrons produced by hitting the moderator surfaces with high-energy β rays reduce their speed in the moderator interspace by random-direction successive collisions. Only electrons reaching the end of the W ribbon at the earthed-grid side are accelerated by the grid–moderator potential (E_{acc}), because this potential does not affect charged particles inside the narrow moderator interspace. The moderator interspace is long and narrow (about 10:1) in our case. It is valid to say, in our W-ribbon geometry, that $E_\perp$ is not dependent on E_{acc}. For positron beams, the distribution of slow positron emission from a solid surface is peaked in the direction perpendicular to the surface. In addition, the probability of re-emission of slow positrons by successive collisions is very low. In a long and narrow moderator interspace, only slow positrons with small $E_\perp$ are accelerated by E_{acc}. This moderator ribbon geometry results in rather good conditions for slow-electron production, but poor conditions for slow-positron emission.

Unfortunately, for positron beams the energy scale correction by the addition of $E_\perp$ was not performed due to the lack of an energy standard.

3. Results and discussion

3.1. e^+-CH_4

The total cross sections for positrons with energies less than 20 eV colliding with CH_4 molecules are presented in figure 6, along with the experimental results of Charlton *et al* (1983), Kauppila *et al* (1983)†, Floeder *et al* (1985), and the theoretical data of Jain and Thompson (1983). The present results were obtained by averaging the preliminary results (Sueoka and Mori 1984b) and the new measurements. Three theoretical curves were based on the 'AT' potential of Jain and Thompson (1982), the 'BC' potential of Burke and Chandra (1972) and the 'GT' potential of Gianturco and Thompson (1976). The present data in the low-energy range were not explained by these theoretical curves, though the GT curve has a similar trend to the present data, while the data of Charlton *et al* (1983) coincide fairly well with the AT curve. As shown in the figure, the present data coincide very well with those of Kauppila *et al* (1983). The minimum, $Q^+_{min} = (4.8 \pm 0.4) \times 10^{-16}$ cm^2, was presented at 4.5 eV, while $Q^+_{min} = 3.4 \times 10^{-16}$ cm^2 at 5.2 eV in the data of Charlton *et al* and $Q^+_{min} = 4.8 \times 10^{-16}$ cm^2 at 5 eV in the data of Kauppila *et al*. The minimum is very shallow. Though the experimental data have the same minimum position, values of the total cross section in the present data and in the data of Kauppila *et al* are much higher than those of Charlton *et al* in the range below the threshold of positronium formation, E_{Ps}. The increase of total cross sections in the vicinity of E_{Ps} with increasing positron energy corresponds mainly to the positronium formation cross sections which were directly

† Data of Kauppila *et al* were read from their small figure, so there may be errors in their data in figures 6 and 7.

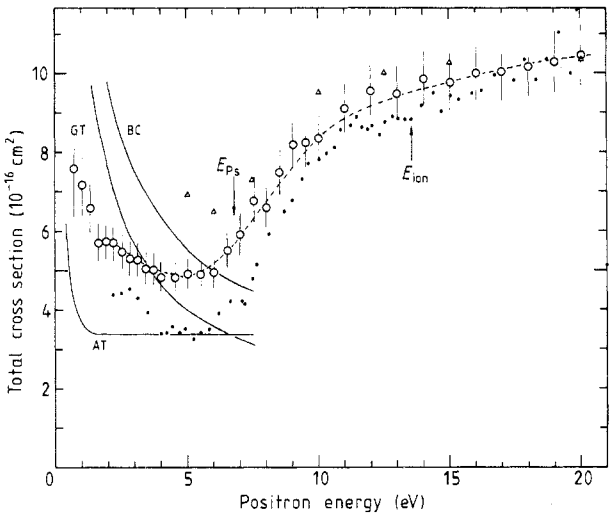

Figure 6. Total cross sections for positrons colliding with methane at low energies. Experimental points: ○, this experiment; ●, Charlton *et al* (1983); - - -, Kauppila *et al* (1983); △, Floeder *et al* (1985). Theoretical curves: ——, AT, GT and BC from Jain and Thompson (1983). Error bars show uncertainties of the present results except the error due to forward scattering. Thresholds for positronium formation and ionisation are indicated by arrows.

observed by Griffith (1984). If the present data are used instead of the data of Charlton *et al* (1983), to estimate the absolute positronium formation cross section values in methane gas the absolute values decrease by about 20% due to the difference in the minimum value. In the energy range at the threshold of ionisation, the values of the total cross section are in good agreement with those of Charlton *et al* (1983) and Kauppila *et al* (1983). On the other hand, the data of Floeder *et al* (1985) below 10 eV are higher than the other data.

As shown in figure 3, the data below 3 eV indicate that the cross section values are shifted to about 10–25% higher than those given in figure 6 when corrected for the effect of forward scattering. The effect is due to the increase of sharp forward scattering by rotation excitations. The shifted values tend towards the GT theoretical curve.

Values of total cross sections for positrons in the range from 10 to 400 eV are depicted in figure 7 with the data of Charlton *et al* (1980, 1983), Kauppila *et al* (1983) and Floeder *et al* (1985). The present data and the data of Kauppila *et al* and Floeder *et al* coincide well in this range. In the energy range from 30 to 400 eV, the data show the typical decrease of the cross section with increasing impact energy.

3.2. e^--CH_4

Studies of electron collisions with CH_4 molecules have been performed by measurements of total absorption cross sections (Brode 1925, Brüche 1927, 1930, Ramsauer and Kollath 1930, Barbarito *et al* 1979, Kauppila *et al* 1983, Ferch *et al* 1985, Jones 1985), differential cross sections (Tanaka *et al* 1982, 1983, Sohn *et al* 1983, Müller *et al* 1985), diffusion experiments (Duncan *et al* 1972), dissociation experiments (Winters 1975), and theoretical works (Gianturco and Thompson 1976, Jain and Thompson 1982, 1983). Values of total cross sections for electrons with energies lower than 20 eV

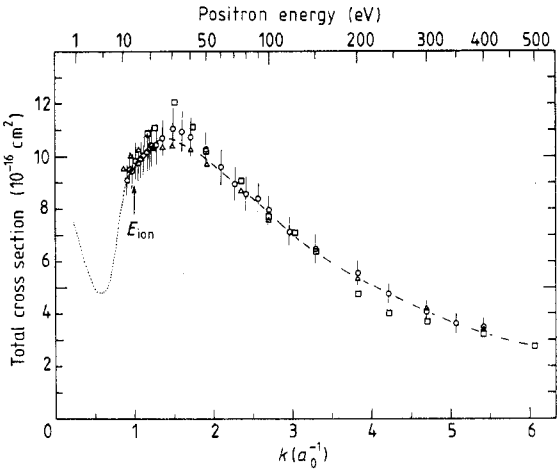

Figure 7. Total cross sections for positrons colliding with methane extending to intermediate energies. Experimental points: ○, this experiment; □, Charlton *et al* (1983); - - -, Kauppila *et al* (1983); △, Floeder *et al* (1985). The dotted curve gives a visual fitting curve of the present data. The arrow indicates the threshold of ionisation.

are shown in figure 8, along with the data of Ferch *et al* (1985), Jones (1985), Kauppila *et al* (1983), Barbarito *et al* (1979), Brüche (1927), the experimental integrated elastic cross section of Tanaka *et al* (1983) and the theoretical data of Gianturco and Thompson (1976) and Jain and Thompson (1982). On the whole, the data are in disagreement. In the energy range below 5 eV the present data coincide with those of Ferch *et al* (1985), but do not show the Ramsauer minimum for lack of measured energy range.

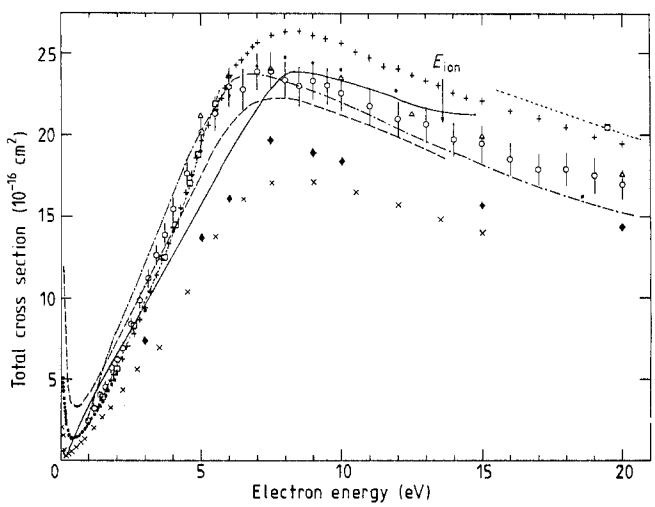

Figure 8. Total cross sections for electrons colliding with methane at low energies. Experimental results: ○, this experiment; ●, Ferch *et al* (1985); △, Floeder *et al* (1985); - -□ - -, Kauppila *et al* (1983); +, Jones (1985); ×, Barbarito *et al* (1979); — · —, Brüche (1927); ◆, integrated elastic cross section of Tanaka *et al* (1983). Theoretical results: ——, AT from Jain and Thompson (1982); - - -, Gianturco and Thompson (1976). The arrow shows the threshold of ionisation.

Values of the total cross section for electrons in higher energy ranges are given in figure 9, together with the experimental results of Kauppila *et al* (1983), Floeder *et al* (1985) and Jones (1985). The total cross section curves for electrons in the range from 20 to 100 eV do not coincide with each other. The present data coincide well with those of Floeder *et al* above 100 eV.

In comparison with the data in figure 7, the total cross section curves for electrons and positrons coincide in the range from 150 to 400 eV, as shown in the measurement of $e^{\pm}$-He (Kauppila *et al* 1981). On the other hand, in the data of Kauppila *et al* (1983) and Floeder *et al* (1985), the curve for e^{-}-CH_4 is higher than those for e^{+}-CH_4, as is the case for many other gases. Cross section values for our group for electron collisions are generally lower than those of the Wayne State University group.

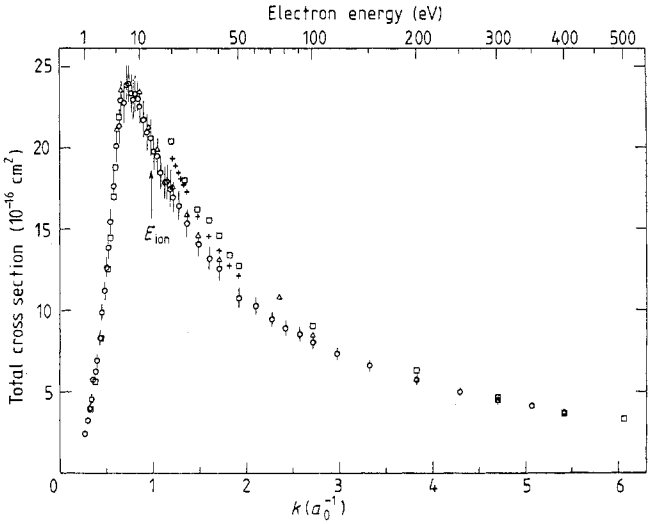

Figure 9. Total cross sections for electrons colliding with methane extending to intermediate energies. Experimental points: ○, this experiment; △, Floeder *et al* (1985); □, Kauppila *et al* (1983); +, Jones (1985).

3.3. $e^{\pm}$-C_2H_4 and $e^{\pm}$-C_2H_6

Measurements of the total cross section for $e^{\pm}$-ethylene and $e^{\pm}$-ethane are presented. Values for positron collisions at energies less than 20 eV are shown in figure 10 with the experimental data of Floeder *et al* (1985) and the present data for e^{+}-CH_4. The minima in the total cross section are distinctly shown; $Q^{+}_{min} = (13.1 \pm 1.3) \times 10^{-16}$ cm^2 at 4.0 eV for C_2H_4 and $Q^{+}_{min} = (10.6 \pm 1.1) \times 10^{-16}$ cm^2 at 3.4 eV for C_2H_6. The minimum for C_2H_4 is not considered to be the Ramsauer minimum, because the threshold of positronium formation, E_{Ps}, exists in the minimum region. For C_2H_6, the minimum is observed as in CH_4. In the range below 3 eV, the values of the total cross sections increase with decreasing impact energy, as do those for e^{+}-CH_4 and e^{+}-CO_2. The checks for the effect of forward scattering, such as shown in figures 3 and 4 for CH_4, were not performed for C_2H_4 and C_2H_6. On the other hand, the data of Floeder *et al* in the range below 15 eV show a quite different tendency from the present data. A similar trend was shown in figure 6 in the data of Floeder *et al* for e^{+}-CH_4.

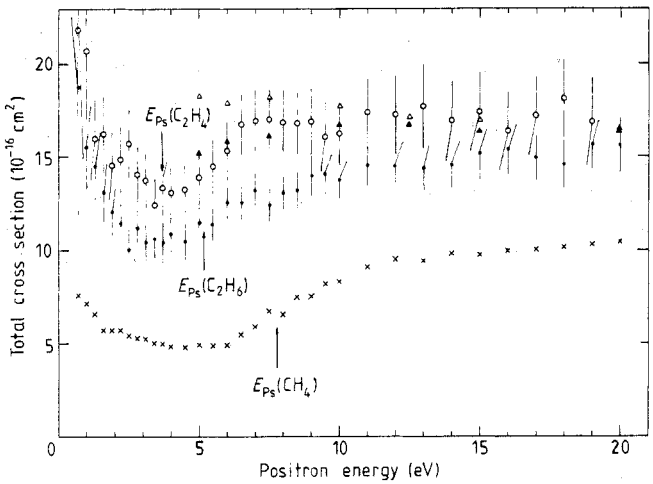

Figure 10. Total cross sections for positrons colliding with ethylene and ethane at low energies. Experimental points: ○ (C_2H_4), ● (C_2H_6), this experiment; △ (C_2H_4), ▲ (C_2H_6), Floeder *et al* (1985). The present data for e^+-CH_4, × are shown for reference. The arrows indicate the threshold of positronium formation.

Values of the total cross section for electrons with energies less than 20 eV are presented in figure 11, together with the data of Brüche (1929, 1930), Floeder *et al* (1985) and the present data for e^--CH_4. For electron collisions, the present data for C_2H_4 and C_2H_6 are in agreement with those of Floeder *et al.* Brüche's experimental curves show discrepancies in parts with the present data. The reason why the peak due to the shape resonance is low and broad is that the energy resolution of electron beams is poor due to the large radial component of the beam.

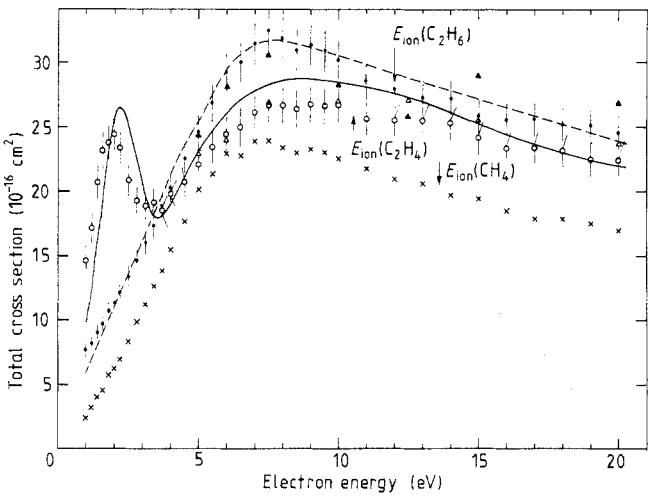

Figure 11. Total cross sections for electrons colliding with ethylene and ethane at low energies. Experimental results: ○ (C_2H_4), ● (C_2H_6), this experiment; △ (C_2H_4), ▲ (C_2H_4) Floeder *et al* (1985); ——, (C_2H_4), Brüche (1927); - - - (C_2H_6), Brüche (1930). The present data for e^--CH_4, × are shown for reference. The thresholds of ionisation are indicated by arrows.

The shape resonance at 1.8 eV and a broad peak at 7.5 eV were reported by Walker *et al* (1978) for the differential cross section measurement of e^--C_2H_4. The energy position of 1.8 eV is lower than the value of 2.2 eV in Brüche's data and 2.0 eV for the present data. As described in the last paragraph of § 2, the energy scale was corrected by the shift of the resonance position in e^--N_2, -CO and -CO_2.

Values of total cross sections for $e^{\pm}$-C_2H_4 in the energy range from 10 to 400 eV are plotted in figure 12 with the experimental data of Floeder *et al* (1985). In figure 13, values of total cross sections for e^+-C_2H_6 and e^--C_2H_6 are also presented with the

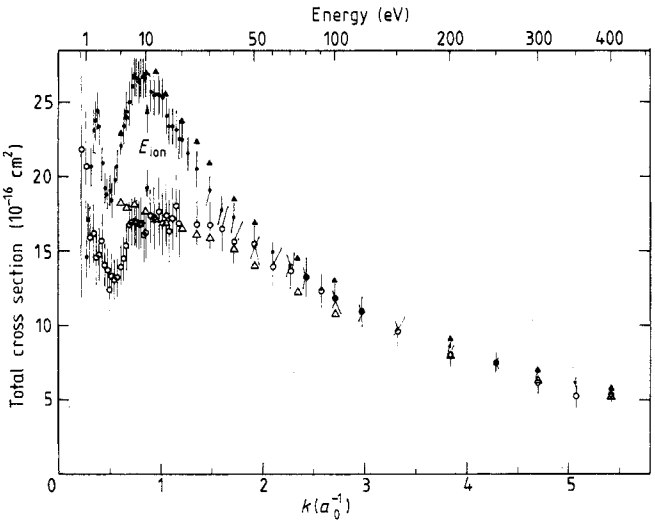

Figure 12. Total cross sections for positrons and electrons colliding with ethylene extending to intermediate energies. Experimental points: ○ e^+ data, ● e^- data, this experiment; △ e^+ data, △ e^- data, Floeder *et al* (1985). The threshold of ionisation is indicated by an arrow.

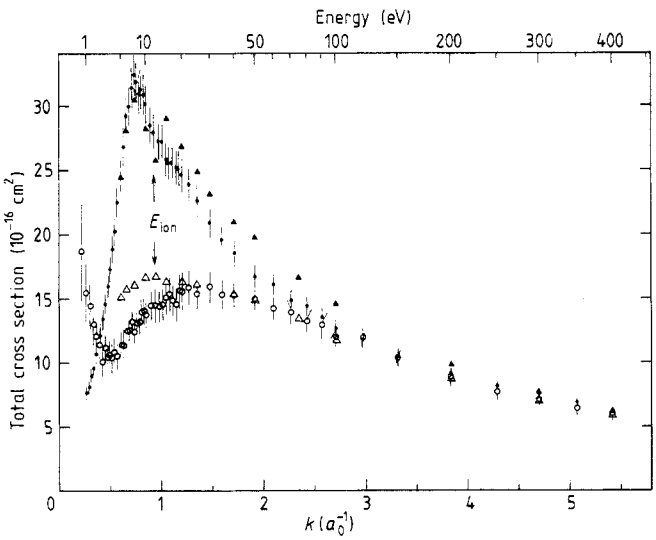

Figure 13. Total cross sections for positrons and electrons colliding with ethane extending to intermediate energies. Experimental points: ○ e^+ data, ● e^- data, this experiment; △ e^+ data; ▲ e^- data, Floeder *et al* (1985). The threshold of ionisation is indicated by an arrow.

Table 1. Total cross sections for positron collisions (10^{-16} cm^2).

Energy (eV)	Methane	Ethylene	Ethane
0.7	7.6 ± 1.2	21.8 ± 9.9	18.7 ± 3.8
1.0	7.1 ± 0.8	20.7 ± 3.7	15.5 ± 2.2
1.3	6.6 ± 0.6	15.9 ± 2.1	14.5 ± 1.8
1.6	5.7 ± 0.5	16.2 ± 2.0	13.1 ± 1.6
1.9	5.7 ± 0.5	14.5 ± 1.8	12.1 ± 1.3
2.2	5.7 ± 0.5	14.8 ± 1.8	11.4 ± 1.1
2.5	5.4 ± 0.4	15.7 ± 1.8	10.0 ± 1.1
2.8	5.3 ± 0.4	14.0 ± 1.5	11.2 ± 1.0
3.1	5.3 ± 0.4	13.7 ± 1.5	10.4 ± 0.9
3.4	5.0 ± 0.4	12.4 ± 1.4	10.6 ± 1.1
3.7	5.0 ± 0.4	13.3 ± 1.5	10.4 ± 1.1
4.0	4.8 ± 0.4	13.1 ± 1.3	10.9 ± 1.0
4.5	4.8 ± 0.4	13.2 ± 1.3	10.5 ± 1.0
5.0	4.9 ± 0.4	13.9 ± 1.5	11.4 ± 0.9
5.5	4.9 ± 0.4	14.5 ± 1.4	11.4 ± 0.9
6.0	4.9 ± 0.4	15.3 ± 1.6	12.5 ± 0.9
6.5	5.5 ± 0.4	16.8 ± 1.6	12.5 ± 0.9
7.0	5.9 ± 0.5	16.9 ± 1.6	13.2 ± 0.9
7.5	6.8 ± 0.5	17.0 ± 1.6	12.4 ± 0.9
8.0	6.6 ± 0.5	16.9 ± 1.6	13.1 ± 0.9
8.5	7.5 ± 0.6	16.8 ± 1.7	13.2 ± 1.0
9.0	7.6 ± 0.6	16.9 ± 1.7	14.0 ± 1.0
9.5	8.2 ± 0.6	16.1 ± 1.8	14.1 ± 1.0
10.0	8.3 ± 0.6	16.2 ± 1.6	13.8 ± 1.0
11.0	9.1 ± 0.6	17.4 ± 1.8	14.5 ± 1.1
12.0	9.5 ± 0.6	17.2 ± 2.1	14.5 ± 1.3
13.0	9.4 ± 0.7	17.7 ± 2.3	14.4 ± 1.2
14.0	9.9 ± 0.7	16.9 ± 2.1	14.6 ± 1.3
15.0	9.8 ± 0.7	17.4 ± 2.1	15.1 ± 1.3
16.0	10.0 ± 0.7	16.3 ± 2.1	15.4 ± 1.3
17.0	10.0 ± 0.8	17.2 ± 2.1	14.9 ± 1.2
18.0	10.1 ± 0.7	18.1 ± 2.1	14.6 ± 1.3
19.0	10.3 ± 0.8	16.9 ± 2.3	15.6 ± 1.3
20.0	10.4 ± 0.8		15.6 ± 1.5
22.0	10.5 ± 0.8		15.9 ± 1.3
25.0	10.7 ± 0.7	16.8 ± 1.6	15.4 ± 1.2
30.0	11.1 ± 0.8	16.8 ± 1.6	16.0 ± 1.2
35.0	10.9 ± 0.8	16.5 ± 1.5	15.3 ± 1.1
40.0	10.7 ± 0.7	15.6 ± 1.4	15.3 ± 0.9
50.0	10.3 ± 0.7	15.5 ± 1.4	15.0 ± 0.9
60.0	9.6 ± 0.7	14.0 ± 1.3	14.3 ± 0.9
70.0	9.0 ± 0.6	13.6 ± 1.2	14.0 ± 0.9
80.0	8.6 ± 0.6	13.3 ± 1.3	13.3 ± 0.8
90.0	8.4 ± 0.6	12.3 ± 1.1	13.0 ± 1.0
100	8.0 ± 0.6	11.9 ± 1.0	12.0 ± 0.8
120	7.1 ± 0.5	11.0 ± 1.0	12.0 ± 0.8
150	6.5 ± 0.6	9.6 ± 1.0	10.4 ± 0.7
200	5.5 ± 0.5	8.0 ± 0.8	8.9 ± 0.7
250	4.8 ± 0.4	7.5 ± 0.6	7.7 ± 0.6
300	4.1 ± 0.4	6.2 ± 0.8	7.1 ± 0.5
350	3.6 ± 0.3	5.2 ± 0.8	6.4 ± 0.5
400	3.5 ± 0.4	5.4 ± 0.5	6.0 ± 0.5

Table 2. Total cross sections for electron collisions (10^{-16} cm^2).

Energy (eV)	Methane	Ethylene	Ethane
1.0	2.4 ± 0.2	14.6 ± 1.2	7.7 ± 0.5
1.2	3.2 ± 0.2	17.1 ± 1.1	8.1 ± 0.5
1.4	4.1 ± 0.3	20.7 ± 1.3	9.0 ± 0.5
1.6	4.6 ± 0.3	23.1 ± 1.4	9.7 ± 0.6
1.8	5.7 ± 0.3	23.8 ± 1.3	10.7 ± 0.6
2.0	6.2 ± 0.4	24.5 ± 1.3	11.4 ± 0.7
2.2	6.9 ± 0.4	23.4 ± 1.2	12.1 ± 0.7
2.5	8.3 ± 0.5	20.9 ± 1.1	13.4 ± 0.8
2.8	9.8 ± 0.5	19.3 ± 1.0	14.7 ± 0.8
3.1	11.2 ± 0.6	18.8 ± 1.0	16.0 ± 0.8
3.4	12.5 ± 0.6	19.1 ± 1.1	17.3 ± 0.9
3.7	13.8 ± 0.7	18.5 ± 1.2	18.9 ± 1.1
4.0	15.5 ± 0.8	19.8 ± 1.0	20.3 ± 1.1
4.5	17.6 ± 0.9	20.7 ± 1.1	22.5 ± 1.1
5.0	20.1 ± 1.0	22.1 ± 1.1	24.6 ± 1.2
5.5	21.3 ± 1.1	23.4 ± 1.2	26.9 ± 1.3
6.0	22 9 ± 1.2	24.4 ± 1.3	29.2 ± 1.4
6.5	22.8 ± 1.3	25.0 ± 1.5	30.0 ± 1.5
7.0	23.9 ± 1.1	26.1 ± 1.3	31.4 ± 1.6
7.5	23.9 ± 1.2	26.7 ± 1.3	32.5 ± 1.7
8.0	23.4 ± 1.2	26.7 ± 1.3	31.8 ± 1.6
8.5	23.0 ± 1.2	26.4 ± 1.4	30.9 ± 1.5
9.0	23.3 ± 1.1	26.7 ± 1.3	31.3 ± 1.6
9.5	23.0 ± 1.1	26.6 ± 1.3	30.9 ± 1.6
10.0	22.5 ± 1.1	26.7 ± 1.3	30.2 ± 1.5
11.0	21.7 ± 1.1	25.7 ± 1.3	28.5 ± 1.4
12.0	21.0 ± 1.1	25.5 ± 1.3	27.9 ± 1.5
13.0	20.6 ± 1.1	25.5 ± 1.3	27.3 ± 1.4
14.0	19.7 ± 1.0	25.3 ± 1.3	27.2 ± 1.3
15.0	19.4 ± 1.1	24.1 ± 1.2	25.9 ± 1.3
16.0	18.5 ± 1.0	23.4 ± 1.2	25.6 ± 1.3
17.0	17.9 ± 0.9	23.4 ± 1.2	25.6 ± 1.2
18.0	17.9 ± 1.0	23.2 ± 1.3	25.3 ± 1.3
19.0	17.5 ± 1.1	22.5 ± 1.3	25.2 ± 1.4
20.0	17.0 ± 0.9	22.5 ± 1.2	24.6 ± 1.3
22.0	16.4 ± 0.9	21.6 ± 1.1	23.9 ± 1.2
25.0	15.3 ± 0.9	20.5 ± 1.2	22.6 ± 1.3
30.0	14.1 ± 0.7	19.1 ± 1.0	20.9 ± 1.1
35.0	13.2 ± 0.7	17.7 ± 0.9	19.6 ± 1.0
40.0	12.6 ± 0.7	17.2 ± 1.0	18.5 ± 1.1
50.0	10.8 ± 0.6	15.3 ± 0.7	16.7 ± 0.9
60.0	10.3 ± 0.5	14.9 ± 0.7	16.1 ± 0.8
70.0	9.4 ± 0.5	14.0 ± 0.7	15.0 ± 0.8
80.0	8.9 ± 0.4	13.2 ± 0.7	14.5 ± 0.7
90.0	8.5 ± 0.4	12.6 ± 0.6	13.6 ± 0.7
100	8.0 ± 0.4	11.8 ± 0.6	12.7 ± 0.6
120	7.3 ± 0.4	10.9 ± 0.5	11.8 ± 0.6
150	6.6 ± 0.3	9.8 ± 0.5	10.5 ± 0.5
200	5.7 ± 0.3	8.6 ± 0.4	9.2 ± 0.5
250	5.0 ± 0.2	7.5 ± 0.4	8.2 ± 0.4
300	4.4 ± 0.2	6.9 ± 0.3	7.6 ± 0.4
350	4.1 ± 0.2	6.2 ± 0.3	6.9 ± 0.3
400	3.7 ± 0.2	5.7 ± 0.3	6.2 ± 0.3

data of Floeder *et al.* As for CH_4, the curves for the positron and electron collisions in figures 12 and 13 almost coincide with each other above 60 eV, while the data of Floeder *et al* show a difference between electron and positron collisions.

3.4. Comparison: C_2H_4 against C_2H_6

As mentioned in § 1, we are interested in the effect of the C=C double bond in C_2H_4 on the total cross section. The electronic orbits in ethane molecules are saturated, as in methane, but not saturated in ethylene. For comparison of the data for C_2H_4 with those for C_2H_6, subtraction for the positron and electron collisions was attempted.

At low energies, the difference $Q_t^-(C_2H_4)-Q_t^-(C_2H_6)$ is large because of the shape resonance of C_2H_4 in the range. On the other hand, the difference curve $Q_t^+(C_2H_4)-Q_t^+(C_2H_6)$ for positron collisions shows a peak at 7 eV. This peak corresponds to a small hump in the curve of the total cross section for e^+-C_2H_4 shown in figure 10. It is not understood whether the hump is caused by an abnormal increase of positronium formation or a kind of resonance. The measurement of the energy dependence of positronium formation cross sections for the C_2H_4 molecule is expected. Moreover, measurements of the total cross section in C_2H_2 molecules, with a triple bond, are also expected, in which a very large shape resonance was observed in electron collisions. In positron collisions $Q_t^+(C_2H_4) > Q_t^+(C_2H_6)$ was observed below about 30 eV. This has been also shown in the data of Floeder *et al* (1985). At higher energies the results of total cross sections for positrons and electrons are roughly understandable as the difference between ionisation cross sections for these molecules. Values of the cross sections at different energies are given in tables 1 and 2.

Acknowledgments

The authors would like to thank Professor Hiroshi Tanaka for valuable discussion on electron collisions and Yasunao Katayama for his helpful assistance in various aspects of this work.

References

Barbarito E, Basta M, Calicchio M and Tessari G 1979 *J. Chem. Phys.* **71** 54-9
Brode R B 1925 *Phys. Rev.* **25** 636-44
Brüche E 1927 *Ann. Phys., Lpz* **83** 1065-107
—— 1929 *Ann. Phys., Lpz* **2** 909-32
—— 1930 *Ann. Phys. Lpz* **4** 387-408
Burke P G and Chandra N 1972 *J. Phys. B: At. Mol. Phys.* **5** 1696-711
Charlton M, Griffith T C, Heyland G R and Wright G L 1980 *J. Phys. B: At. Mol. Phys.* **13** L353-6
—— 1983 *J. Phys. B: At. Mol. Phys.* **16** 323-41
Duncan C W and Walker I C 1972 *J. Chem. Soc.* **68** 1514-21
Ferch J, Granitza B and Raith W 1985 *J. Phys. B: At. Mol. Phys.* **18** L445-50
Floeder K, Fromme D, Raith W, Schwab A and Sinapius G 1985 *J. Phys. B: At. Mol. Phys.* **18** 3347-59
Gianturco F A and Thompson D G 1976 *J. Phys. B: At. Mol. Phys.* **12** L383-5
Griffith T C 1979 *Adv. At. Mol. Phys.* **15** 135-66
—— 1984 *Positron Scattering in Gases* ed J W Humberston and M R C McDowell (New York: Plenum) pp 53-63

Hoffman K R, Dababneh M S, Hsieh Y-F, Kauppila W E, Pol V, Smart J H and Stein T S 1982 *Phys. Rev.* A **25** 1393-403

Jain A 1983 *J. Chem. Phys.* **78** 6579-83

Jain A and Thompson D G 1982 *J. Phys. B: At. Mol. Phys.* **15** L631-7

—— 1983 *J. Phys. B: At. Mol. Phys.* **16** 1113-23

Jones R K 1985 *J. Chem. Phys.* **82** 5424-7

Kauppila W E, Dababneh M S, Hsieh Y-F, Kwan Ch K, Smith S J, Stein T S and Uddin M N 1983 *Proc. 13th Int. Conf. on the Physics of Electronic and Atomic Collisions (Berlin)* ed J Eichler, W Fritsch, V Hertel, N Stolterfoht and U Wille (Amsterdam: North-Holland) Abstracts p 303

Kauppila W E and Stein T S 1982 *Can. J. Phys.* **60** 471-93

Kauppila W E, Stein T S, Smart J H, Dababneh M S, Ho Y K, Dowing J P and Pol V 1981 *Phys. Rev.* A **24** 725-42

Mizogawa T, Nakayama Y, Kawaratani T and Tosaki M 1985 *Phys. Rev.* A **31** 2171-9

Müller R, Jung K, Kochem K-H, Sohn W and Ehrhardt H 1985 *J. Phys. B: At. Mol. Phys.* **18** 3971-85

Ramsauer C and Kollath R 1930 *Ann. Phys., Lpz* **4** 91-108

Sohn W, Jung K and Ehrhardt H 1983 *J. Phys. B: At. Mol. Phys.* **16** 891-901

Sueoka O 1982 *J. Phys. Soc. Japan* **51** 2381-2

Sueoka O and Mori S 1984a *J. Phys. Soc. Japan* **53** 2491-500

—— 1984b *At. Collisions Res. Japan* **10** 12-6

Tanaka H, Kubo M, Onodera N and Suzuki A 1983 *J. Phys. B: At. Mol. Phys.* **16** 2861-9

Tanaka H, Okada T O, Boesten L, Suzuki T, Yamamoto T and Kubo M 1982 *J. Phys. B: At. Mol. Phys.* **15** 3305-19

Walker I C, Stamatovic A and Wong S G 1978 *J. Chem. Phys.* **69** 5532-7

Winters H F 1975 *J. Chem. Phys.* **63** 3462-6